ID Design Press, Skopje, Republic of Macedonia
Open Access Macedonian Journal of Medical Sciences. 2019 Nov 15; 7(21):3546-3553.
https://doi.org/10.3889/oamjms.2019.850
eISSN: 1857-9655
Basic Science

Preparation of In Situ Cross-Linked N-Maleoyl Chitosan-Oxidized Sodium Alginate Hydrogels for Drug Delivery Applications

Subur P. Pasaribu[1, 2], Jamaran Kaban[1*], Mimpin Ginting[1], Jansen Silalahi[3]

[1]Department of Chemistry, Faculty of Mathematics and Natural Sciences, Universitas Sumatera Utara, Medan-20155, Indonesia; [2]Department of Chemistry, Faculty of Mathematics and Natural Sciences, Mulawarman University, Samarinda-75123, Indonesia; [3]Department of Pharmaceutical Chemistry, Faculty of Pharmacy, Universitas Sumatera Utara, Medan-20155, Indonesia

Citation: Pasaribu SP, Kaban J, Ginting M, Silalahi J. Preparation of In Situ Cross-Linked N-Maleoyl Chitosan-Oxidized Sodium Alginate Hydrogels for Drug Delivery Applications. Open Access Maced J Med Sci. 2019 Nov 15; 7(21):3546-3553. https://doi.org/10.3889/oamjms.2019.850

Keywords: In situ; Schiff base; MCS-OSA hydrogels; Physicochemical; Drug delivery

***Correspondence:** Jamaran Kaban. Department of Chemistry, Faculty of Mathematics and Natural Sciences, Universitas Sumatera Utara, Medan-20155. E-mail: jamaran.kaban@usu.ac.id

Received: 21-Aug-2019; **Revised:** 24-Sep-2019; **Accepted:** 25-Sep-2019; **Online first:** 14-Oct-2019

Funding: The research was financially supported by the Directorate of Higher Education, Ministry of Research Technology and High Education Indonesia

Competing Interests: The authors have declared that no competing interests exist

Abstract

AIM: This study was aimed to prepare in situ cross-linked N-maleoyl chitosan – oxidised sodium alginate (MCS – OSA) hydrogel loaded with metronidazole (MTZ) for drug delivery applications.

METHODS: The hydrogel was prepared by in situ cross-linking via Schiff base reaction between amine (-NH2) groups from MCS and aldehyde (-CHO) groups from OSA at the different ratio, and the MTZ was loaded into the hydrogels along with the gelatin processes.

RESULTS: The highest drug entrapment efficiency (DEE) was exhibited by MTZ-H3 (5: 5) with DEE of 99.20% and a gel fraction of 97.52%. FTIR results revealed that Schiff base reaction was occurred by the absorption peak of –C = N- groups at 1628 cm^{-1} and indicated that there is insignificant alteration at different ratio of MCS and OSA. The best sustained of in vitro release profiles of MTZ was shown by MTZ-H3, which is 74.92% and 75.65% at pH 1.2 and 7.4 for 12 h of release, respectively.

CONCLUSION: The optimised ratio between MCS and OSA to prepare in situ cross-linked hydrogels were found to be 5:5 according to the results of DEE and in vitro drug release profiles of MTZ and the MTZ loaded MCS-OSA hydrogels have a great potential which can be applied in biomedical applications.

Introduction

Polysaccharide-based polymer hydrogels such as cellulose, chitosan, starch, alginate, dextrin and it's derivatives have attracted attention of researchers for drug delivery applications which can be controlled and applied at specific sites owing to the ease of preparation, good encapsulation properties of variation drugs, good biocompatibility and responsive to external stimulant [1], [2], [3], [4], [5]**.** Smart and controllable based drug delivery hydrogels considered as a preferable alternative which can improve in decreasing the dosage and side effects compared to the single unit release of tablet [6], [7]. However, the applications of chitosan in controllable drug delivery systems are limited due to its solubility [8], [9], [10]. Hence, to enhance the solubility of chitosan in water and different pH of aqueous solutions, modification by amine ($-NH_2$) and hydroxyl (-OH) functional groups were conducted as reported in Mohamed and Fahmy (2012) [11] and Wang et al., (2016) [12] works, such as acylation of chitosan for N-maleoyl chitosan (MCS) preparation.

MCS can be synthesized via acylation of maleoyl group to N-terminal in glucosamine chitosan unit. Recently, the utilisation of chitosan derivative such as MCS in polymer-based drug delivery has drawn the attention of researchers besides using pristine chitosan. Some advantages of MCS are non-toxic, degradable, good hydrophilicity and biocompatibility which also soluble in any medium at different pH. The solubility of MCS depends on the degree of substitution of maleoyl in water and

physiological pH [13], [14], [15]. Therefore, in this research, MCS was assumed to be cross-linked with natural bifunctional cross-linking agents (e.g. dialdehyde alginate) and *in situ* hydrogel can be obtained.

Oxidised sodium alginate can be prepared by oxidation reaction using oxidising agents (periodic acid or sodium periodate) to oxidise 2,3-O-dihydroxyl alginate for dialdehyde alginate preparation [12]. The OSA has been widely used as natural macromolecule cross-linking agent for hydrogels preparation due to the minimum or non-toxic properties which can replace the relatively toxic chemical cross-linking (e.g. formaldehyde, acetaldehyde and glutaraldehyde) [16]. Also, OSA has good biodegradable and intrinsic biochemical characteristics such as good solubility in a variation of pH, containing aldehyde functional groups, abundant nature, and ease of covalently cross-linking.

Several studies have reported synthesising *in situ*-forming hydrogels via Schiff base covalent cross-linking without any chemical cross-linking agents between modified-chitosan derivative and dialdehyde alginate. For example, *in situ*-forming hydrogels via Schiff base covalent cross-linking between $–NH_2$ groups from N, O-carboxymethyl chitosan and –CHO groups from OSA containing silver nanoparticles (AgNPs) for antibacterial and bioactive compound delivery applications has been published by Fan et al., (2011) [17]. The N, O-carboxymethyl chitosan/oxidised alginate hydrogels containing BSA [18], curcumin and nano curcumin [19], RGD-grafted oxidised sodium alginate–N-succinyl chitosan-based for bone tissue engineering [20], hydroxypropyl chitosan and sodium alginate dialdehyde for the reconstruction of the corneal endothelium [2].

In this study, MTZ loaded MCS-OSA hydrogel is prepared through *in situ* Schiff base reaction between amine ($-NH_2$) groups from MCS and aldehyde (-CHO) groups from OSA which has not been reported before and the schematic reaction is illustrated in Figure 1. Moreover, the effects of the different ratio between MCS and OSA on physicochemical properties, drug entrapment efficiency (DEE) and *in vitro* drug release profiles of MTZ including the kinetic modelling at pH 1.2 and 7.4 were evaluated.

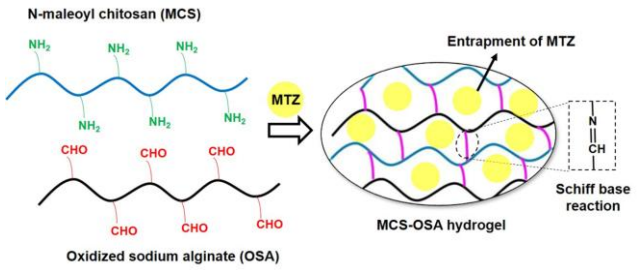

Figure 1: Schematic of in situ drug loading in MCS-OSA hydrogels via Schiff base cross-linking reaction

Material and Method

Materials

The materials used in this experiment were N-maleoyl chitosan (MCS) (degree of substitution = 0.66) and oxidized sodium alginate (OSA) (aldehyde contents = 7.43 mmol/g) which were synthesized according to our previous research [21], [22], HCl, NaCl, phosphate buffer solution (PBS) (pH 7.4) and metronidazole (MTZ) was a gift from PT. Kimia Farma Plant Bandung Indonesia. All chemicals were used as received without further treatment.

Preparation of MCS-OSA hydrogels

MCS and OSA were dissolved separately in 0.1 M PBS solution (pH 7.4) with a desired concentration of 2% (w / v). Then, each solution of MCS and OSA were mixed at room temperature at a different ratio which is abbreviated as H1 (9: 1), H2 (7: 3), H3 (5: 5), H4 (3: 7), and H5 (1: 9). Before the characterisation, the obtained hydrogels were washed several times by distilled water, followed by drying for further characterisation [23], [24], [25].

Preparation of in situ MTZ loading in MCS-OSA hydrogels

MTZ-MCS-OSA hydrogel was fabricated by dissolving an amount of 25 mg MTZ in a total volume of 10 ml mixture solution of MCS-OSA at room temperature. Initially, MTZ was mixed well in MCS solution before mixing between MCS and OSA at a different ratio. Then, the obtained MTZ-MCS-OSA hydrogels were dried for further analyses and oxidised [23], [24], [25].

FTIR analysis

Samples were analysed as a powder mixed with KBr powder by Fourier transform infrared (FTIR) method. Spectra were collected in the wavenumber of 4000-400 cm^{-1}, a scan number of 64 and a resolution of 4 cm^{-1} using a Shimadzu IR Tracer-100 spectrometer.

The surface morphology of hydrogels was observed with a ZEISS EVO MA10 (Germany) at an accelerating voltage of 10 kV and magnification of 1000 x. Before the scanning process, the hydrogels were dried to prevent the shrinkage of samples and then coated by a thin layer of platinum through the sputtering method.

XRD analysis

The crystallinity of prepared hydrogels was determined using a Bruker D2 Phaser X-ray

diffractometer at 2Θ = 10-70° (scanning rate = 6°/min) in Cu Kα radiation (λ =0.151418 nm) with a working voltage of 30 kV and current of 10 mA.

Physiochemical properties of MCS-OSA hydrogels

In this study, physicochemical properties comprise of gel-forming time, gel fraction and swelling ratio (both pH 1.2 and 7.4) of the H1-H5 hydrogels.

Gel forming time

Gel forming time was observed visually at room temperature while the mixture solution of MCS and OSA losing the fluidity from viscous solution to elastic (rubber) or solid phase. The time when the solution turns to solid than was recorded as gel-forming time [23].

Gel fraction

The samples (Wo) were immersed in 50 mL distilled water for 24 h until equilibrium swelling was achieved, to remove the soluble parts MCS-OSA in the hydrogels. Afterwards, the hydrogels were dried at 50°C in the oven and reweighed (We). The gel fraction (GF) was performed in triplicate and calculated by the following equation [23]:

$$GF(\%)= \frac{We}{Wo} \times 100\% \quad (1)$$

Swelling ratio

The swelling experiments were conducted in solution pH 1.2 and pH 7.4 separately. The hydrogels were immersed in 50 ml of each solution at 37°C, then weighed (Ws) at a certain time interval (1-360 min) until equilibrium swelling was achieved. The swelling ratio (SR) was conducted in triplicate and determined by the following equation [23], [26]:

$$SR(\%)= \frac{Ws-We}{We} \times 100\% \quad (2)$$

Determination of drug entrapment efficiency (DEE)

The drug entrapment efficiency (DEE) of MTZ-MCS-OSA hydrogels was determined by the extraction method. 50 mg of the MTZ-MCS-OSA hydrogels was dispersed in 0.1 M PBS solution (pH 7.4) and stirred at 37 ± 0.5°C for 24 h. Then, the solution was filtered and diluted for UV-Vis spectrophotometer analysis at a wavelength of 320.6 nm. The determination of DEE was conducted in triplicate to ensure their reproducibility of results and data are presented as mean ± standard deviation (SD). The drug entrapment efficiency (DEE) was calculated by the following equation [24], [25].

$$DEE\ (\%)= \frac{EDL}{TDL} \times 100\%$$

Where EDL and TDL denote the experimental drug loading and theoretical drug loading of MTZ in the hydrogels, respectively. Then, the entrapment of MTZ in MCS-OSA hydrogels was abbreviated as MTZ-Hnhydrogels, which Hn denotes as H1 to H5 hydrogels.

In vitro release profiles of drug-loaded hydrogels

In vitro release profiles of MTZ-MCS-OSA hydrogels (H1-H5) were determined in two different pH environment which are 1.2 (0.1 N HCl solution) and 7.4 (0.1 M PBS solution) [24], [25] by using USP paddle method dissolution with a speed of 50 rpm and total volume of 900 ml at temperature of 37 ± 0.5°C [27]. After certain time intervals between 0 and 12 h, aliquots (5 ml) of the sample solution were taken from the release medium, and an equivalent amount of fresh 0.1 N HCl solution was added to maintain a constant volume. The taken solution was then diluted and the concentration of MTZ was analysed by UV-Vis spectrophotometer at the wavelength of 277 nm for pH 1.2. The same procedure was also used to carry out to determine the *in vitro* release profiles of MTZ-MCS-OSA hydrogels (H1-H5) in pH 7.4 solution and the wavelength of UV-Vis spectrophotometer analysis was at 320.6 nm. The drug release experiments were conducted in triplicate to ensure their reproducibility of results and data are presented as mean ± standard deviation (SD).

Statistical analysis

All measured data are expressed as mean ± standard deviation (S.D.) and performed using Origin software, version 8.6 and Kruskal-Wallis test with a value of $p < 0.05$ which was considered to indicate the statistical significance.

Results

FTIR Analysis

As shown in Figure 2, the absorption peak at the wavelength of 3448.72 cm^{-1} presented in the spectra of MCS attribute to stretching vibration of –OH and $–NH_2$ which is overlapping, meanwhile weak absorption at 2931.80 cm^{-1} wavelength correspond to stretching vibration of C-H [23],[28]. The vibration of C = O from maleic anhydride acid in the chitosan backbone indicated by the absorption peak at 1712.79

$cm^{-1}$and also confirmed by C = O vibration of amide groups at 1558.48 cm^{-1}. Moreover, at 825.53 cm^{-1} is attributed to C = C groups in maleoyl [13], [29]. Hence, the characterisation by FTIR revealed that the synthesised compound is N-maleoyl chitosan (MCS).

On the other hand, FTIR spectra of OSA, the free –OH, intramolecular and non-oxidized intermolecular bonding are evidenced by broaden peak at 3471.87 cm^{-1}. Afterwards, the absorption peaks at 2939.52 and 1405.18 cm^{-1} are stretching vibration of aldehyde (-CHO) groups [23]. At the wavelength of 1627.92 cm^{-1} is referred to C = O stretching vibration of aldehyde functional groups which resulted from the oxidation of –OH. Moreover, the formation of hemiacetal (aldehyde) was proved by the absorption band of C-O-C (cyclic ether) at 1033.85 cm^{-1} [24]. The absorption peaks at 794.67 and 732.95 cm^{-1} are referred to C-H groups which contributed to bond-breaking of C-C in OSA.

All FTIR spectrums of hydrogels (H1-H5) showed the insignificant difference as represented in Figure 2. The stretching vibration of –OH at 3464.15 cm^{-1} revealed the intermolecular hydrogen bonds [25]. The presence of characteristic peak of hemiacetal formation at 864.11 cm^{-1} is due to stretching vibration of –C-N- a bond which also considered as the coupling reaction between –CHO from OSA and $–NH_2$ from MCS [25]. In addition, the absorption peak at 1627.92 cm^{-1} confirmed the formation of –C = N- groups (Schiff base or imine) [25], [30], [31].

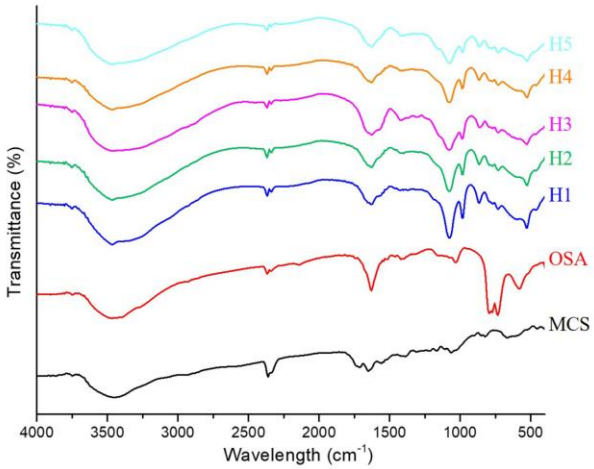

Figure 2: FTIR spectrum of MCS, OSA and MCS-OSA hydrogels at different ratio (H1-H5)

SEM analysis

The images of SEM (magnification: 1000 x) were depicted in Figure 3 and indicated that Schiff base cross-linking exhibited the presence of rough and dense surface of all MCS-OSA hydrogels (H1-H5). However, the surface morphology of all hydrogels (H1-H5) showed an insignificant difference.

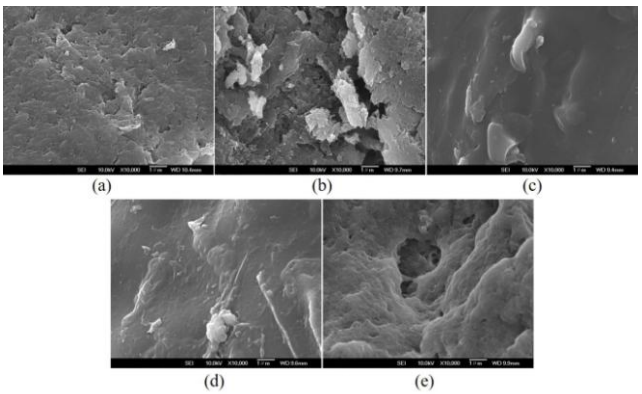

Figure 3: SEM images of MCS-OSA hydrogels: A) H1; B) H2; C) H3; D) H4; and E) H5 at magnification of 1000 x

XRD analysis

The diffraction patterns indicated the amorphous structure of the hydrogels. All of the hydrogels exhibited a broad peak at 2□= 21° which is attributed to the networks of hydrogels as shown in Figure 4 and the results showed insignificant alteration at the different ratio between MCS and OSA.

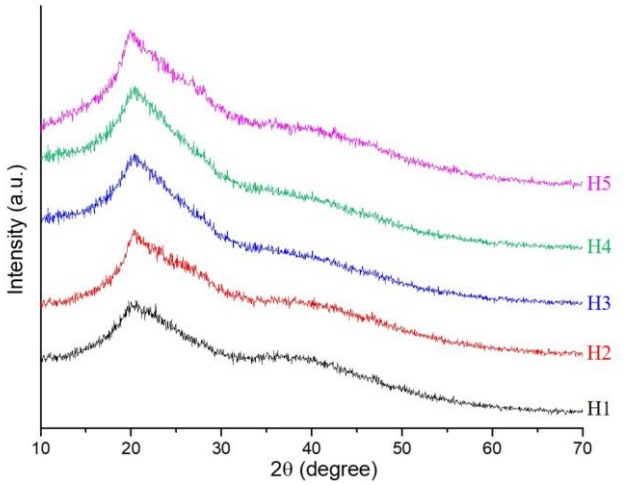

Figure 4: XRD patterns for MCS-OSA hydrogels at different ratio (H1-H5)

Gel forming time

Gel forming time (gelation time) of H1-H5 were observed and determined at room temperature when both mixtures of MCS and OSA underwent cross-linking (gelation) to form hydrogels. The gel-forming time for H1-H5 varied between 4.51 and 23.52 min as represented in Table 1.

With increasing ratio of MCS from H1 to H3, the ability to cross-link to create hydrogel network was faster because at high concentration of MCS, more -NH_2 groups reacted with –CHO groups from OCS. Moreover, H4 and H5 showed drastically slow gelation time due to the saturation of aldehyde groups at a high ratio of OCS and led to the hindrance of cross-

linking [17]. Similar results were also obtained in the study reported by Kamoun (2016) [23] and described that the faster gelation time of succinyl chitosan-dialdehyde starch (SCS-DAS) hydrogel was obtained at a higher amount of SCS.

Table 1: The result of gelation time of MCS-OSA hydrogels at different ratio (H1-H5)

Samples	Gel forming time (min)
H1	4.51 ± 0.02
H2	5.18 ± 0.02
H3	7.49 ± 0.02
H4	19.44 ± 0.02
H5	23.52 ± 0.03

*(n = 3, ± SD).

Gel fraction

The gel fraction increased from 81.72-97.52% for H1-H3 and decreased to 55.13% and 12.58% for H4 and H5, as shown in Table 2. As mentioned earlier, for H4 and H5, the saturation of aldehyde groups was occurred and hindered the cross-linking therefore decrease the gel fraction. Besides, the results of the gel fraction are linearly related to the cross-linking density of hydrogel and indicated that the highest cross-linking density was possessed by H3.

Table 2: The result of gel fraction of MCS-OSA hydrogels at different ratio (H1-H5)

Samples	Gel fraction (%)
H1	81.72 ± 0.06
H2	85.03 ± 0.02
H3	97.52 ± 0.04
H4	55.13 ± 0.05
H5	12.58 ± 0.04

*(n = 3, ± SD).

The swelling ratio of hydrogels

The swelling ratio (SR) of the hydrogels at pH 1.2 (0.1 N HCl solution) and pH 7.4 (0.1 M PBS solution) was shown in Figure 5(a) and (b), respectively which plotted as a function of time. At pH 1.2 (0.1 N HCl solution), the swelling ratio of H1, H2 and H3 hydrogels increased from 86.5% to 120.68% and 141.42%. In correlation with gel fraction, high gel fraction resulted in high cross-linking density and limited the mobility of polymer chains, therefore, decrease the swelling properties. At the same time, the hydrophilic groups, -COOH of MCS also can contribute to hydrating more water molecules.

Meanwhile, after adding OSA, the C = N bonds (Schiff base reaction) was formed for the gelation between –CHO from MCS and $–NH_2$ from OSA which enhance the hydrophobicity. Therefore, at high concentration of OSA, the hydrophobicity of hydrogels increased and fewer hydrogen bonds of hydrogel with H_2O was formed.

On the other hand, H4 possessed low gel fraction to compare to H1, H2 and H3. Thus the swelling properties of H4 increased [17]. Moreover, the swelling ratio of H4 at the interval time of 120-360 minutes of immersion showed a drastically decline from 168.98% to 119.71% which is due to the unstable and easily degraded networks [24]. Furthermore, such a phenomenon was also occurred for H5 and has been degraded at a swelling time of 90 minutes.

On the other hand, a similar trend was observed between the results of swelling ratio in pH 1.2 and pH 7.4. Nevertheless, the swelling ratio at pH 7.4 increased drastically compared to pH 1.2, and this could be owing to the higher electrostatic repulsion of interpolymer and interpolymer chain which resulted in more expanding networks of hydrogel [25]. Besides, at higher pH, the swelling ability was higher for the polymer containing anionic (-COOH) groups [28]. Afterwards, the phenomenon of degradation and unstable network was also obtained for H4 and H5 at pH 7.4.

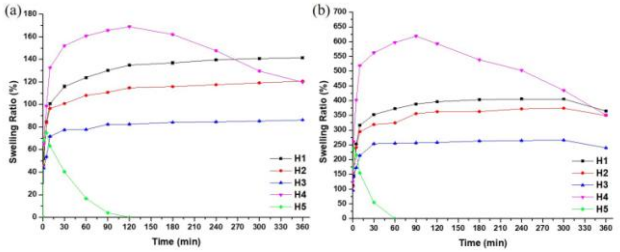

Figure 5: Swelling ratio profiles of MCS-OSA hydrogels at: A) pH 1.2; B) pH 7.4 (n = 3, ± SD).

Determination of drug entrapment efficiency (DEE)

The results of drug entrapment efficiency (DEE) of MTZ-MCS-OSA hydrogels (H1-H5), including the experimental drug loading (EDL) are summarised in Table 3 and represented in Figure 6. The results of drug entrapment efficiency (DEE) of hydrogels varied between 84.76% and 99.22%, where the highest DEE was possessed by MTZ-H3 hydrogels. Since the MTZ-MCS-OSA hydrogels were prepared via *in situ* cross-linking (Schiff base), during the cross-linking processes, the MTZ is entrapped in the networks of the hydrogel. Therefore, higher gel fraction exhibited the highest DEE.

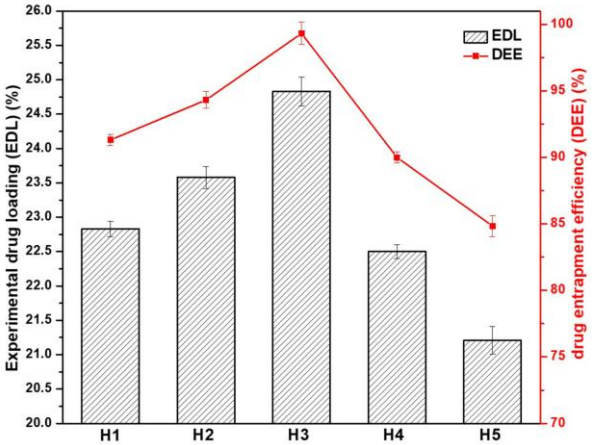

Figure 6: Drug entrapment efficiency (DEE) of MTZ-MCS-OSA hydrogel (n = 3, ± SD)

In vitro drug release and kinetic modelling

The *in vitro* release profiles of MTZ-MCS-OSA hydrogels (H1-H5) in both pH 1.2 (0.1 N HCl solution) and pH 7.4 (0.1 M PBS solution) at 37 ± 0.5°C are presented in Figure 7 (a) and (b), respectively. The cumulative release of MTZ-MCS-OSA hydrogels (H1-H5) at pH 1.2 for 60 min was determined to be 68.68, 63.37, 22.57, 81.66 and 87.50%, respectively. The burst release (burst effect) was exhibited by all hydrogels except MTZ-H3 hydrogel and indicated the release profiles of MTZ-MCS-OSA hydrogels were depended significantly on the composition of MCS and OSA [23], [33], [34], [35].

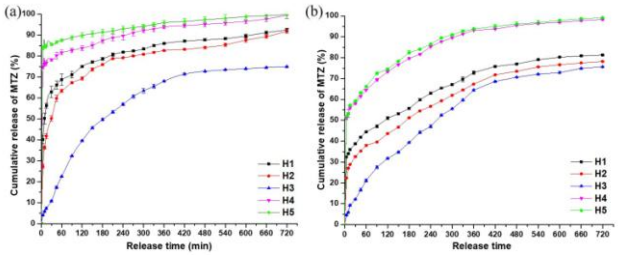

Figure 7: The release profiles of MTZ-MCS-OSA hydrogels at: (a) pH 1.2; (b) pH 7.4 (n = 3, ± SD)

On the other hand, a more delayed pattern of drug release profiles was obtained for MTZ-H3 hydrogel, and the cumulative release for 1 h in pH 1.2 medium was 22.57%. Similarly, the drug release was found to be sufficiently sustained for 12 h of release, with cumulative release of 74.92%, while the cumulative release of MTZ-MCS-OSA (H1, H2, H4 and H5) varied between 91-99% which also indicated that MTZ-H3 hydrogel possessed retentive properties for drug delivery system.

Table 3: The release parameter values obtained by fitting *in vitro* release data to Higuchi and Korsmeyer-Peppas release models at pH 1.2

Release systems	Cumulative release (%)			Higuchi		Korsmeyer-Peppas		
	2h	6h	12h	$k_H(h^{-0.5})$	R^2	$K_p(h^{-0.5})$	n	R^2
MTZ-H1	75.06	86.03	92.44	4.54	-	38.07	0.14	0.99
MTZ-H2	69.38	82.64	91.86	4.35	0.29	27.02	0.19	0.97
MTZ-H3	39.59	67.98	74.92	3.27	0.95	4.29	0.45	0.95
MTZ-H4	83.83	93.85	99.49	5.01	-	64.12	0.06	0.99
MTZ-H5	89.90	95.87	99.81	5.18	-	75.69	0.04	0.99

*The negative R^2 values were obtained from the Higuchi model fitting to release data of MTZ in MCS-OSA hydrogels.

The synthesized *in situ* drug-loaded MCS-OSA hydrogels released MTZ at a higher rate in pH 1.2 (0.1 N HCl solution) compared to the release in pH 7.4 (0.1 M PBS solution). It is because the solubility of MTZ is higher at pH 1.2 (64.8 mg/mL at room temperature) than in pH values between 2.5 and 8.0 (10 mg/ml) [36], [37], [38].

To further determine the mechanisms involved in drug release from the hydrogels, the *in vitro* release data in pH 1.2 and 7.4 were fitted using Higuchi [39] and Korsmeyer-Peppas [40] release model by nonlinear least-squares regression analysis using the Origin software as shown in Figure 8.

Table 4: The release parameter values obtained by fitting *in vitro* release data to Higuchi and Korsmeyer-Peppas release models at pH 7.4

Release systems	Cumulative release (%)			Higuchi		Korsmeyer-Peppas		
	2h	6h	12h	$k_H(h^{-0.5})$	R^2	$K_p(h^{-0.5})$	n	R^2
MTZ-H1	51.00	72.85	81.27	3.70	0.61	17.88	0.23	0.98
MTZ-H2	43.60	67.35	78.19	3.43	0.82	11.78	0.29	0.99
MTZ-H3	31.77	64.37	75.65	3.06	0.98	2.72	0.52	0.98
MTZ-H4	73.25	93.15	98.32	4.78	0.01	35.52	0.16	0.99
MTZ-H5	74.53	93.72	99.14	4.85	-	36.77	0.15	0.99

*The negative R^2 values were obtained from the Higuchi model fitting to release data of MTZ in MCS-OSA hydrogels.

The models including the coefficient of determination (R^2) are presented in Table 3 and Table 4, respectively.

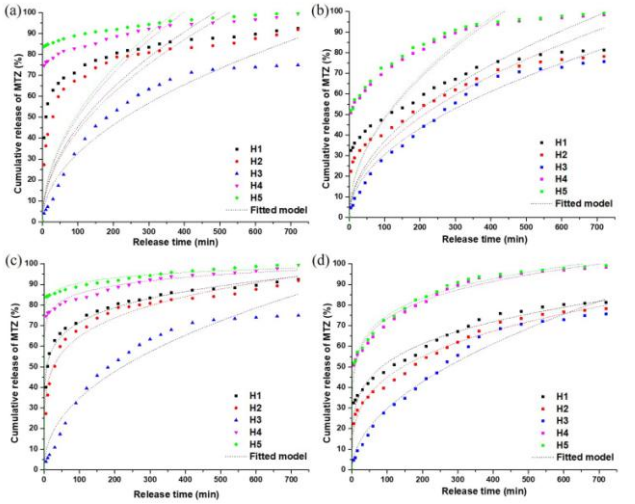

Figure 8: The fitted release profiles of Higuchi model at A) pH 1.2; B) pH 7.4 and Korsmeyer-Peppas model at C) pH 1.2; D) pH 7.4 to release MTZ in MCS-OSA hydrogels (n = 3, ± SD)

Discussion

The results of *in vitro* release data at pH 1.2 indicated that the Higuchi release model only can be used to describe the release profiles of MTZ-H3 hydrogels with R^2 value = 0.95 while poor R^2 value (0.29) was obtained for MTZ-H2 hydrogels and the release profiles of MTZ-H1, MTZ-H4 and MTZ-H5 were failed to be described by Higuchi model, as indicated by negative R^2 values.

Furthermore, Korsmeyer-Peppas release model (pH 7.4) showed good agreement between the experimental data and model predictions with high R^2 values ranging from 0.95-0.99. Likewise, good fitting was also showed by Korsmeyer-Peppas release model with R^2 ranged from 0.98-0.99 of *in vitro* release data at pH 7.4. Besides, the *in vitro* release data at pH 7.4 fitted by Higuchi model showed that the R^2 values of H1, H2 and H3 are 0.61, 0.82 and 0.98, respectively and the model failed to fit H4 and H5 *in vitro* release data, as indicated by negative R^2 values. Moreover, only MTZ-H3 hydrogels in pH 7.4 release medium showed exponent n factor n values of 0.52

which the mechanism was governed by anomalous (non-Fickian) transport (0.45 < n < 1.00). Other than that, the n values of all MTZ-MCS-OSA hydrogels at both pH 1.2 and 7.4 were less than or equal to 0.45 (n ≤ 0.45) and confirmed the drug release mechanism is Fickian diffusion [41].

In conclusion, *in situ* MTZ-loaded MCS-OSA hydrogel has been successfully synthesized by utilizing MCS and OSA at different ratio (H1-H5) via Schiff base cross-linking reaction and the time of gelation varied between 4.51 and 23.52 min. On the other hand, increasing ratio of OSA from H1 to H3 showed increasing in gel fraction and decreases for further increasing (H4 and H5). On the contrary with gel fraction, the swelling ratio increased linearly with increasing ratio of MCS. In brief, MTZ-H3 hydrogels possessed the highest gel fraction and DEE as well. Moreover, the drug release mechanism of all release systems is governed by Fickian diffusion except for MTZ-H3 which is anomalous transport (non-Fickian diffusion). Therefore, this MTZ-MCS-OSA hydrogel potentially can be applied in drug delivery system.

Acknowledgement

The authors were gratefully thanked to Directorate of Higher Education, Ministry of Research Technology and High Education Indonesia for financial support in the study.

References

1. Bajpai SK, Bajpai M, Shah FF. Alginate dialdehyde (AD)-crosslinked casein films: Synthesis, characterization and water absorption behavior. Des Monomers Polym. 2016; 19(5):406-19. https://doi.org/10.1080/15685551.2016.1169374

2. Liang Y, Liu W, Han B, Yang C, Ma Q, Song F, et al. An in situ formed biodegradable hydrogel for reconstruction of the corneal endothelium. Colloids Surfaces B Biointerfaces. 2011; 82(1):1-7. https://doi.org/10.1016/j.colsurfb.2010.07.043 PMid:20832263

3. Reddy GV, Reddy NS, Nagaraja K, Rao KSV. Synthesis of pH Responsive Hydrogel Matrices from Guar gum and Poly(acrylamide-co-acrylamidoglycolicacid) for Anti-Cancer Drug Delivery. J Appl Pharm Sci. 2018; 8(8):84-91. https://doi.org/10.7324/JAPS.2018.8813

4. Rottensteiner U, Sarker B, Heusinger D, Dafinova D, Rath S, Beier J, et al. In vitro and in vivo Biocompatibility of Alginate Dialdehyde/Gelatin Hydrogels with and without Nanoscaled Bioactive Glass for Bone Tissue Engineering Applications. Materials (Basel). 2014; 7(3):1957-74. https://doi.org/10.3390/ma7031957 PMid:28788549 PMCid:PMC5453292

5. Yan S, Wang T, Li X, Jian Y, Zhang K, Li G, et al. Fabrication of injectable hydrogels based on poly(l -glutamic acid) and chitosan. RSC Adv. 2017; 7(28):17005-19. https://doi.org/10.1039/C7RA01864A

6. Almeida H, Amaral MH, Lobão P. Temperature and pH stimuli-responsive polymers and their applications in controlled and selfregulated drug delivery. J Appl Pharm Sci. 2012; 2(6):01-10.

7. Sun X, Shi J, Xu X, Cao S. Chitosan coated alginate/poly(N-isopropylacrylamide) beads for dual responsive drug delivery. Int J Biol Macromol. 2013; 59:273-81. https://doi.org/10.1016/j.ijbiomac.2013.04.066 PMid:23628584

8. Bashir S, Teo YY, Ramesh S, Ramesh K, Khan AA. N-succinyl chitosan preparation, characterization, properties and biomedical applications: a state of the art review. Rev Chem Eng. 2015; 31(6):563-97. https://doi.org/10.1515/revce-2015-0016

9. Hu D, Wang H, Wang L. Physical properties and antibacterial activity of quaternized chitosan/carboxymethyl cellulose blend films. LWT - Food Sci Technol. 2016; 65:398-405. https://doi.org/10.1016/j.lwt.2015.08.033

10. Tzaneva D, Simitchiev A, Petkova N, Nenov V, Stoyanova A, Denev P. Synthesis of Carboxymethyl Chitosan and its Rheological Behaviour in Pharmaceutical and Cosmetic Emulsions. J Appl Pharm Sci. 2017; 7(10):70-8.

11. Mohamed NA, Fahmy MM. Synthesis and Antimicrobial Activity of Some Novel Cross-Linked Chitosan Hydrogels. Int J Mol Sci. 2012; 13(9):11194-209. https://doi.org/10.3390/ijms130911194 PMid:23109847 PMCid:PMC3472739

12. Wang CH, Liu WS, Sun JF, Hou GG, Chen Q, Cong W, et al. Non-toxic O-quaternized chitosan materials with better water solubility and antimicrobial function. Int J Biol Macromol. 2016; 84(December 2015):418-27. https://doi.org/10.1016/j.ijbiomac.2015.12.047 PMid:26712700

13. Fan J, Chen J, Yang L, Lin H, Cao F. Preparation of dual-sensitive graft copolymer hydrogel based on N-maleoyl-chitosan and poly(N-isopropylacrylamide) by electron beam radiation. Bull Mater Sci. 2009; 32(5):521-6. https://doi.org/10.1007/s12034-009-0077-x

14. Vanichvattanadecha C, Supaphol P, Rujiravanit R. Preparation and physico-chemical characteristics of W-maleoyl chitosan films. Macromol Symp. 2008; 264(1):121-6. https://doi.org/10.1002/masy.200850419

15. Zhu A, Lu Y, Yingnan P, Dai S, Wu H. Self-assembly of N-maleoylchitosan in aqueous media. Colloids Surfaces B Biointerfaces. 2009; 76(1):221-5. https://doi.org/10.1016/j.colsurfb.2009.10.040 PMid:19939640

16. Xu Y, Li L, Yu X, Gu Z, Zhang X. Feasibility study of a novel crosslinking reagent (alginate dialdehyde) for biological tissue fixation. Carbohydr Polym. 2012; 87(2):1589-95. https://doi.org/10.1016/j.carbpol.2011.09.059

17. Fan LH, Pan XR, Zhou Y, Chen LY, Xie WG, Long ZH, et al. Preparation and characterization of crosslinked carboxymethyl chitosan-oxidized sodium alginate hydrogels. J Appl Polym Sci. 2011; 2011. https://doi.org/10.1002/app.34041

18. Li X, Kong X, Zhang Z, Nan K, Li L, Wang X, et al. Cytotoxicity and biocompatibility evaluation of N, O-carboxymethyl chitosan/oxidized alginate hydrogel for drug delivery application. Int J Biol Macromol. 2012; 50(5):1299-305. https://doi.org/10.1016/j.ijbiomac.2012.03.008 PMid:22465755

19. Li X, Chen S, Zhang B, Li M, Diao K, Zhang Z, et al. In situ injectable nano-composite hydrogel composed of curcumin, N,O-carboxymethyl chitosan and oxidized alginate for wound healing application. Int J Pharm. 2012; 437(1-2):110-9. https://doi.org/10.1016/j.ijpharm.2012.08.001 PMid:22903048

20. Liu X, Peng W, Wang Y, Zhu M, Sun T, Peng Q, et al. Synthesis of an RGD-grafted oxidized sodium alginate-N-succinyl chitosan hydrogel and an in vitro study of endothelial and osteogenic differentiation. J Mater Chem B. 2013; 1(35):4484-92. https://doi.org/10.1039/c3tb20552e

21. Pasaribu SP, Kaban J, Ginting M, Sinaga KR. Synthesis of Dialdehyde Alginate By Oxidation Reaction Sodium Alginate With Sodium Metaperiodate. J Kim Mulawarman. 2017; 14(2):134-8.

22. Pasaribu SP, Kaban J, Ginting M, Sinaga KR. Synthesis and evaluation antibacterial activity of phosphate buffer solution (pH

7.4) - Soluble acylated chitosan derivative. AIP Conf Proc. 2018; 2049. https://doi.org/10.1063/1.5082430

23. Kamoun EA. N-succinyl chitosan-dialdehyde starch hybrid hydrogels for biomedical applications. J Adv Res. 2016; 7(1):69-77. https://doi.org/10.1016/j.jare.2015.02.002 PMid:26843972 PMCid:PMC4703420

24. Tan H, Chu CR, Payne KA, Marra KG. Injectable in situ forming biodegradable chitosan-hyaluronic acid based hydrogels for cartilage tissue engineering. Biomaterials. 2009; 2009. https://doi.org/10.1016/j.biomaterials.2008.12.080 PMid:19167750 PMCid:PMC2676686

25. Yu H, Lu J, Xiao C. Preparation and properties of novel hydrogels from oxidized konjac glucomannan cross-linked chitosan for in vitro drug delivery. Macromol Biosci. 2007; 7(9-10):1100-11. https://doi.org/10.1002/mabi.200700035 PMid:17665410

26. Setiasih S, Prabowo HA, Budianto E, Hudiyono S. Dissolution profiles of partially purified bromelain from pineapple cores [Ananas comosus (L .) Merr] encapsulated in glutaraldehyde-crosslinked chitosan. 2018; 8(10):17-24. https://doi.org/10.7324/JAPS.2018.81003

27. Farshforoush P, Ghanbarzadeh S, Goganian AM, Hamishehkar H. Novel metronidazole-loaded hydrogel as a gastroretentive drug delivery system. Iran Polym J (English Ed. 2017; 26(12):895-901. https://doi.org/10.1007/s13726-017-0575-4

28. Bashir S, Teo YY, Ramesh S, Ramesh K. Synthesis, characterization, properties of N-succinyl chitosan-g-poly (methacrylic acid) hydrogels and in vitro release of theophylline. Polymer (Guildf). 2016; 92:36-49. https://doi.org/10.1016/j.polymer.2016.03.045

29. Hasipoglu HN, Yilmaz E, Yilmaz O, Caner H. Preparation and characterization of maleic acid grafted chitosan. Int J Polym Anal Charact. 2005; 10(5-6):313-27. https://doi.org/10.1080/10236660500479478

30. Nair S, Remya NS, Remya S, Nair PD. A biodegradable in situ injectable hydrogel based on chitosan and oxidized hyaluronic acid for tissue engineering applications. Carbohydr Polym. 2011; 85(4):838-44. https://doi.org/10.1016/j.carbpol.2011.04.004

31. Xu Y, Huang C, Li L, Yu X, Wang X, Peng H, et al. In vitro enzymatic degradation of a biological tissue fixed by alginate dialdehyde. Carbohydr Polym. 2013; 95(1):148-54. https://doi.org/10.1016/j.carbpol.2013.03.021 PMid:23618251

32. Rizwan M, Yahya R, Hassan A, Yar M, Azzahari AD, Selvanathan V, et al. pH sensitive hydrogels in drug delivery: Brief history, properties, swelling, and release mechanism, material selection and applications. Polymers (Basel). 2017; 9(137). https://doi.org/10.3390/polym9040137 PMid:30970818 PMCid:PMC6432076

33. Thomas LM. Formulation and evaluation of floating oral in-situ gel of metronidazole. Int J Pharm Pharm Sci. 2014;

34. Sadeghi M, Soleimani F. Synthesis of Novel Polysaccharide-Based Superabsorbent Hydro Gels Via Graft Copolymerization of Vinylic Monomers onto Kappa-Carrageenan. Int J Chem Eng Appl. 2013; 2(5):304-6. https://doi.org/10.7763/IJCEA.2011.V2.122

35. Majekodunmi S, Akpan E-A. Comparative Study for In-vitro Evaluation of Metronidazole Prepared Using Natural Chitosan from Oyster Shells of Egeria radiata. Br J Pharm Res. 2017; 17(1):1-11. https://doi.org/10.9734/BJPR/2017/33247

36. Rediguieri CF, Porta V, Nunes DS, Nunes TM, Junginger HE, Kopp S, Midha KK, Shah VP, Stavchansky SA, Dressman JB, Barends DM. Rediguieri CF, Porta V, Nunes DSG, Nunes TM, Junginger HE, Kopp S, Midha KK, Shah VP, Stavchansky S, Dressman JB, Barends DM. 2011. Biowaiver monographs for immediate-release solid oral dosage forms: Metronidazole. J Pharm Sci 100: 1618-1627. Journal of Pharmaceutical Sciences. 2011; 100(12). https://doi.org/10.1002/jps.22787

37. Abid YA, Gustafsson LL, Ericsson O, Hellgren U. Metronidazole in: Handbook of drugs for tropical parasitic infections. Vol. 2 nd ed, Taylor & Francis, 1995:100-105.

38. Wu Y, Fassihi R. Stability of metronidazole, tetracycline HCl and famotidine alone and in combination. 2005; 290:1-13. https://doi.org/10.1016/j.ijpharm.2004.10.015 PMid:15664125

39. Higuchi Takeru. Rate of release of medicaments from ointment bases containing drugs in suspension. J Pharm Sci. 1961; 50(10):874-5. https://doi.org/10.1002/jps.2600501018 PMid:13907269

40. Korsmeyer RW, Gurny R, Doelker E, Buri P, Peppas NA. Mechanisms of solute release from porous hydrophilic polymers. Int J Pharm. 1983; 15(1):25-35. https://doi.org/10.1016/0378-5173(83)90064-9

41. Ritger PL, Peppas NA. A simple equation for description of solute release I.Fickian and non -Fickian release from non-swellable device in the form of slabs, spheres, cylinders or discs. J Control Release. 1987; 5:23-36. https://doi.org/10.1016/0168-3659(87)90034-4